PACAP deficiency aggravates atherosclerosis in ApoE deficient mice

Erik Rasbach[a,1], Paul Splitthoff[a,1], Gabriel A. Bonaterra[a,*], Anja Schwarz[a], Lilli Mey[a], Hans Schwarzbach[a], Lee E. Eiden[b], Eberhard Weihe[c], Ralf Kinscherf[a]

[a] Department of Medical Cell Biology, Institute for Anatomy and Cell Biology, Medical Faculty, Philipps-University of Marburg, Robert-Koch-Str. 8, 35037 Marburg, Germany
[b] Section on Molecular Neuroscience, Laboratory of Cellular and Molecular Regulation, National Institute of Mental Health Intramural Research Program, Bethesda, 20814 MD, USA
[c] Department of Molecular and Cellular Neuroscience, Institute for Anatomy and Cell Biology, Medical Faculty, Philipps-University of Marburg Robert-Koch-Str. 8, 35037 Marburg, Germany

ARTICLE INFO

ABSTRACT

Pituitary Adenylate Cyclase-Activating Polypeptide (PACAP) plays an important role in cytoprotection, inflammation and cardiovascular regulation. Thus, we studied the involvement of PACAP in atherogenesis. Differentiated human THP-1 macrophages (MΦ) were stimulated with oxidized low-density lipoproteins (oxLDL) and the influence of PACAP38 treatment on lipid content and TNF release was determined. To test the effect of PACAP deficiency (PACAP$^{-/-}$) on the development of atherosclerosis under standard chow (SC) or cholesterol-enriched diet (CED) *in vivo*, PACAP$^{-/-}$ mice were crossbred with ApoE$^{-/-}$ to generate PACAP$^{-/-}$/ApoE$^{-/-}$ mice. Blood cholesterol and triglyceride levels were quantified. Lumen stenosis in the brachiocephalic trunk, cellularity and amounts of pro-inflammatory as well as autophagy-, apoptosis- and necroptosis-relevant proteins were analysed in atherosclerotic plaques by quantitative immunohistochemistry. *In vitro*, PACAP38 inhibited oxLDL-induced intracellular lipid storage as well as TNF release in MΦ. *In vivo*, after SC, but not under CED, PACAP$^{-/-}$/ApoE$^{-/-}$ mice showed an increased lumen stenosis compared to ApoE$^{-/-}$ mice. In atherosclerotic plaques of PACAP$^{-/-}$/ApoE$^{-/-}$ mice, the immunoreactive areas of TNF$^+$, IL-1β$^+$, autophagic, apoptotic and necroptotic cells were increased. In contrast, the overall cell density was decreased compared to ApoE$^{-/-}$ under SC, while no differences were seen under CED. Similar plasma cholesterol levels were observed in PACAP$^{-/-}$/ApoE$^{-/-}$ and ApoE$^{-/-}$ mice under the respective feeding regime. Thus, PACAP$^{-/-}$/ApoE$^{-/-}$ mice represent a novel mouse model of accelerated atherosclerosis where CED is not required. Our data indicate that PACAP acts as an endogenous atheroprotective neuropeptide. Thus, stable PACAP agonists may have potential as anti-atherosclerotic therapeutics. The specific PACAP receptor(s) mediating atheroprotection remain(s) to be identified.

1. Introduction

Pituitary adenylate cyclase activating polypeptide (PACAP) is a neuropeptide with multifunctional anti-inflammatory and cytoprotective properties (Vaudry et al., 2009; Miyata et al., 1989). PACAP has been associated with a variety of physiological and pathophysiological processes related to neuroprotection, control of energy metabolism and impact on respiratory and cardiovascular system (Diané et al., 2014). As PACAP and its specific PAC1 receptor have been found in cardiac tissue and blood vessels (Nandha et al., 1991; Gasz et al., 2006), PACAP signaling has been suggested to play an important role in the cardiovascular system and to represent a potential target for future therapeutic applications. PACAP exists as two α-amidated peptides of 38 (PACAP38) or 27 (PACAP27) amino acids (Harmar et al., 1998) and is a key player in neuroendocrine circuits under stress by activating the hypothalamic-pituitary adrenal and the splanchnic-adrenomedullary axes (Hamelink et al., 2002; Holgert et al., 1996; Stroth et al., 2011). Moreover, PACAP mediates inhibition of proliferation, cytoprotection

of endothelial cells (EC) and smooth muscle cells (SMC) as well as reduction of lipid peroxides produced by EC and SMC under hyperlipidemia, suggesting possible anti-atherosclerotic potential (Chang, 1997). Furthermore, the PACAP receptors (PAC1, VPAC1, VPAC2) have been reported to be expressed by macrophages (MΦ) and various other cell types (Delgado et al., 1999; Ganea and Delgado, 2001; Waschek, 2013), suggesting immunomodulatory effects of PACAP signaling. All three PACAP receptors are involved in the regulation of cAMP generation by coupling to adenylyl cyclases (ACs) with effects on survival, proliferation, differentiation and remodelling (Holighaus et al., 2011; May and Parsons, 2017).

In this context, it is noteworthy that MΦ play a central role during development and progression of atherosclerotic plaques. Thus, PACAP and its receptors may be considered as important regulators of atherogenesis. In this regard, atherosclerosis as a chronic inflammatory disorder leads to plaque formation at distinct sites of the arterial tree through intimal inflammation, necrosis, fibrosis, calcification and after decades of unapparent progression, it might suddenly cause life-threatening syndromes (Bentzon et al., 2014). Characteristic secondary diseases, such as ischemic heart disease and stroke, are the main causes of death worldwide (Libby et al., 2011; Moore and Tabas, 2011). Atherosclerosis is a multifocal disease, which reproducibly develops at distinct regions of the arterial tree (Bentzon et al., 2014). Progression of disease is induced by a complex interaction of chemokines and proinflammatory cytokines as well as subendothelial lipid deposition resulting in hemodynamically relevant lumen stenosis (Bentzon et al., 2014; Moore et al., 2013; Tabas et al., 2007). In this context, hypercholesterolemia and low-density lipoprotein (LDL) cholesterol, and especially oxidized low-density lipoproteins (oxLDL), have been described to play a key role during all stages of the disease.

In spite of extensive research, the precise mechanisms involved in the development and progression of atherosclerotic lesions remain largely unresolved. Therefore, it was the aim of the present study to investigate in cell culture, whether PACAP alters atherosclerotic responses of MΦ stimulated with oxLDL and to test in vivo whether PACAP deficiency alters the development and progression of atherosclerosis in ApoE$^{-/-}$ mice fed with standard chow (SC) or cholesterol enriched diet (CED).

2. Methods

2.1. Cell culture

The human leukemic monocyte cell line THP-1 (Leibniz Institute DSMZ, Braunschweig, Germany) was used, being frequently deployed as a model of monocyte/MΦ cell lineage (Tsuchiya et al., 1980). THP-1 cells were cultured in RPMI-1640 medium (Capricorn Scientific GmbH, Ebsdorfergrund, Germany) supplemented with penicillin and streptomycin (Capricorn Scientific GmbH) and 10% fetal bovine serum (Capricorn Scientific GmbH). Cells were cultured at 37 °C in a 5% CO_2 environment with a medium change every 2–3 days. All experiments were performed using cells at passage 9 and lower. THP-1 cells were differentiated into MΦ using 160 nM phorbol 12-mystriate 13-acetate [PMA (Sigma-Aldrich Chemie GmbH, Munich, Germany)] in RPMI 1640 medium for 24 h.

2.2. LDL oxidation

LDL (Cell sciences, Canton, USA) oxidation was performed as previously described by others (Galle and Wanner, 1998; Steinbrecher, 1987). Briefly, the nLDL (native LDL) was suspended in endotoxin-free PBS without Ca^{2+} and Mg^{2+} (LONZA, Ratingen, Germany) to a final concentration of 1 mg protein/ml and dialyzed against PBS using Slide-A-Lyzer Dialysis Cassettes 7K MWCO (Thermo Fisher Scientific Inc., Rockford, USA) and afterwards was oxidized with 50 μM $CuSO_4$ overnight. The reaction was stopped by dialysis against PBS-EDTA. The

grade of oxidation was verified by spectrophotometric analysis (absorbance spectrum between 400 and 600 nm) using a SUNRISE ELISA reader (Tecan, Salzburg, Austria). After oxidative modification, the absorption peaks at 460 and 485 nm, which are characteristic for nLDL, disappeared (Galle and Wanner, 1998). Additionally, oxLDL was analyzed by agarose gel electrophoresis (1% gel) to determine relative electrophoretic mobility (REM). The protein concentrations were determined spectrophotometrically using the Pierce BCA (bicinchoninic acid) Protein Assay (Thermo Fisher Scientific Inc.).

2.3. Oil Red O (ORO) staining

The Oil Red O [ORO (Sigma-Aldrich)] working solution was prepared by diluting the stock solution (3 mg/ml ORO dissolved in 2-propanol) with distilled water (3:2). Afterwards, PMA-differentiated THP-1 MΦ were fixed in 10% PFA, and the ORO working solution was added to the culture dishes. Stained droplets were extracted with 100% isopropanol to quantify intracellular lipids and its absorbance was measured spectrophotometrically at 510 nm. The ORO absorbance was normalised against the crystal violet absorbance measured at 595 nm, reference 660 nm.

2.4. TNF (tumor necrosis factor) release

TNF was determined in the supernatant using the DuoSet-ELISA kit (R&D Systems Europe, Ltd., Abingdon, UK) according to the manufacturer's instructions; 96-well NUNC MaxiSorp™ (Thermo Fisher Scientific Inc.) plates were used. The amount of TNF was normalized with the crystal violet absorbance as described above for ORO.

2.5. Animals

After deletion of PACAP from the PACAP gene locus in C57BL/6 mice (Hamelink et al., 2002), PACAP knockout (Adcyap1$^{-/}$ $^-$/PACAP$^{-/-}$ mice were crossbred with apoliporotein (apo)E knockout (ApoE$^{-/-}$) mice (Charles River, Sulzfeld, Germany) to generate PACAP$^{-/-}$/ApoE$^{-/-}$ mice. Male homozygous PACAP$^{-/-}$/ApoE$^{-/-}$ and ApoE$^{-/-}$ mice were used for the study. At the age of 10 weeks, PACAP$^{-/-}$/ApoE$^{-/-}$ and ApoE$^{-/-}$ mice were fed for 20 weeks either with standard chow (SC, LASQCdiet® Rod16 Rad; LASvendi, Soest, Germany) or with an adjusted-calories cholesterol-enriched diet [CED; "Western type diet" (21% fat, 0.15% cholesterol and 19.5% casein), Altromin GmbH, Lage, Germany]. All animals had ad libitum access to food and water. The procedures were approved by the Regional Commission Gießen (V54-19 c 2015 h 01 MR 20/26 Nr. 21/2014) and were performed in compliance with the regulations for animal experiments at the Philipps-University Marburg.

2.6. Genotyping

Genomic DNA was isolated from the mouse ear using a commercial kit (DNA Extraction Solution; PeqLab, VWR Company, Erlangen, Germany) according to the manufacturer's instructions (DirectPCR® lysis reagent ear; Peqlab, VWR International; Darmstadt, Germany). Subsequently, homozygous transgenic mice were detected by polymerase chain reaction (PCR) using intron-spanning oligonucleotides as shown in Table 1. PCR analysis revealed characteristic single bands for PACAP$^{-/-}$ (310 bp) (Hamelink et al., 2002) and ApoE$^{-/-}$ (245 bp, data not shown).

2.7. Dissection and tissue harvesting

At the age of 30 weeks, the mice were weighed and narcotized and analgized with a combination of ketamine (150 mg/kg) and xylazine (20 mg/kg), the thoracal cavity was opened, and the left ventricular apex was incised and clamped with a cannula. After right atrial incision

Table 1
Oligonucleotides used in the study.

Primer name	Sequence	Amplification Length	Company
PACAP knockout			
PACAP-neoOF	5'-CAC CGG CCT TTA GGG ACC CTT GTA-3'	520bp (+/+)	Eurofins Genomics, Ebersberg, Germany
PACAP-2R	5'-GCT ATT CGG CGT CCT TTG TTT TTA ACC C-3'	520bp + 320bp (+/-)	Eurofins Genomics, Ebersberg, Germany
PACAP-PNT1R	5'-TAG GGG AGG AGT AGA AGG TGG CGC-3'	310bp (-/-)	Eurofins Genomics, Ebersberg, Germany
ApoE knockout			
oIMR180-F	5'-GCC TAG CCG AGG GAG AGC CG-3'	245 bp	Eurofins Genomics, Ebersberg, Germany
oIMR182-R	5'-GCC GCC CCG ACT GCA TCT-3'	245 bp	Eurofins Genomics, Ebersberg, Germany

the vascular system was perfused with a solution consisting of 39 °C warmed phosphate buffered saline (PBS) with 5 Ul/ml heparin (Liquemin® 25000 Ul/5 ml, Roche, Grenzach, Germany), with a delivery volume of 30 ml and a rate of 100 ml/h using an automated syringe-pump (Secura, B. Braun, Melsungen, Germany). Afterwards we injected 250 µl filtered sodium chloride solution (0.9%) + methylene blue (0.25%; Riedel-de Haën, Seelze-Hannover, Germany) into the vascular system. Atherosclerotic processes analogously occurring in advanced human lesions are also seen in the brachiocephalic trunk (BT) of mice (Rosenfeld et al., 2000). The blue colored BT was excised under direct observation through a binocular loupe, embedded in Tissue-Tek® (Sakura Finetek, Stauffen, Germany) and shock-frozen in nitrogen-cooled isopentane. The samples were stored at −80 °C.

2.8. Determination of plasma lipid levels

At the point of opening the right atrium, blood samples were taken, the samples were heparinized (0.25 I.U./ml, Roche) and plasma, obtained by centrifugation (10 min, 650 g), was stored in a −80 °C freezer. Plasma cholesterol and triglyceride levels were analyzed spectrophotometrically using a microplate reader (Sunrise, Tecan, Männedorf, Switzerland) and commercially available kits (cholesterol/ cholesteryl ester quantitation kit ab65359, or triglyceride quantification assay kit ab65336, Abcam, Cambridge, UK), according to the manufacturer's instructions.

2.9. Morphometry and immunohistology

For morphometrical and immunohistological investigations, cryo cross-sectional series (7 µm) of the BTs were performed. The extent of atherosclerotic plaques in the BT and cell density was measured by computer-assisted morphometry. Standard hematoxylin-eosin (HE), Wallart-Houette (WH) and immunhistochemical stains were performed according to methods described earlier (Kinscherf et al., 1997; Romeis, 1989) using antibodies as listed in Table 2. The extent of atherosclerotic lesions was determined by tracing of lumen and plaque areas along the internal elastic lamina (respectively luminal plaque circumference) and computing [(plaque area [µm²])/(lumen area [µm²]) × 100% = lumen stenosis (%)]. Quantification of immunoreactive plaque areas was similarly assessed [(immunoreactive plaque area [µm²])/(total plaque area [µm²]) × 100% = immunoreactive plaque area (%)]. The cell density (no/mm²) of an atherosclerotic plaque was analyzed by counting all cell nuclei per plaque.

2.10. Statistical analyses

All statistical analyses were performed with SigmaPlot 12 (Systat Software Inc., San José, USA). The data were analyzed using Shapiro–Wilk normality test and Brown–Forsythe equal variance test. Statistical significance was determined by the unpaired 2-tailed Students t-test. In case of data failed normality and/or equal variance test, the Mann–Whitney U rank sum test was applied. When appropriate, statistical significance was determined by one-way analysis of variance (ANOVA) with corresponding post-hoc tests. Results are presented as means + standard error of the mean (SEM). The results were considered statistically significant when $p < 0.05$.

3. Results

3.1. PACAP inhibits oxLDL-induced foam cell formation from cultured human MΦs (THP-1 cells)

MΦ are able to internalize and process intracellular lipids to subsequently differentiate into foam cells. By ORO-staining we analyzed in human THP-1 MΦ the intracellular lipid-storage after exposure to oxLDL and measured the effect of PACAP38 addition. We found that lipid storage in human THP-1 MΦ increased 25% ($p < 0.001$) after treatment with 50 µg/ml oxLDL compared to control (Figs. 1A). Treatment of human THP-1 MΦ with 0.1 nM and 10 nM PACAP38 inhibited the oxLDL-induced (50 µg/ml) intracellular lipid storage by 13.6% ($p < 0.01$) and 17.6% ($p < 0.001$), respectively (Fig. 1A).

Table 2
Antibodies used in the study.

Name	Number	Company	Dilution
Goat anti-rabbit IgG HRP	ZRH1158	Linaris, Dossenheim, Germany	1:200–1:500
Goat anti-rat IgG HRP	STAR72	AbD Serotec, Düsseldorf, Germany	1:100
Rabbit anti-mouse APG5L/ATG5	ab 64227	Abcam, Cambridge, UK	1:100
Rabbit anti-mouse cleaved caspase-3 (Asp175)	9661	Cell Signaling/NEB, Frankfurt, Germany	1:600
Rabbit anti-mouse cyclooxygenase 2	ab 15191	Abcam, Cambridge, UK	1:300
Rabbit anti-mouse IL-1-beta	ab 9722	Abcam, Cambridge, UK	1:100
Rabbit anti-mouse IL-6	ab 6672	Abcam, Cambridge, UK	1:500
Rabbit anti-mouse Ki67	ab 15580	Abcam, Cambridge, UK	1:250
Rabbit anti-mouse RIP3	ab 56164	Abcam, Cambridge, UK	1:125
Rabbit anti-mouse smooth muscle α-actin	ab 5694	Abcam, Cambridge, UK	1:500
Rabbit anti-mouse TNF	ab 6671	Abcam, Cambridge, UK	1:50
Rat anti-mouse CD68	MCA 1957	AbD Serotec, Düsseldorf, Germany	1:100

HRP indicates horseradish peroxidase; IL, interleukin; TNF, tumor necrosis factor.
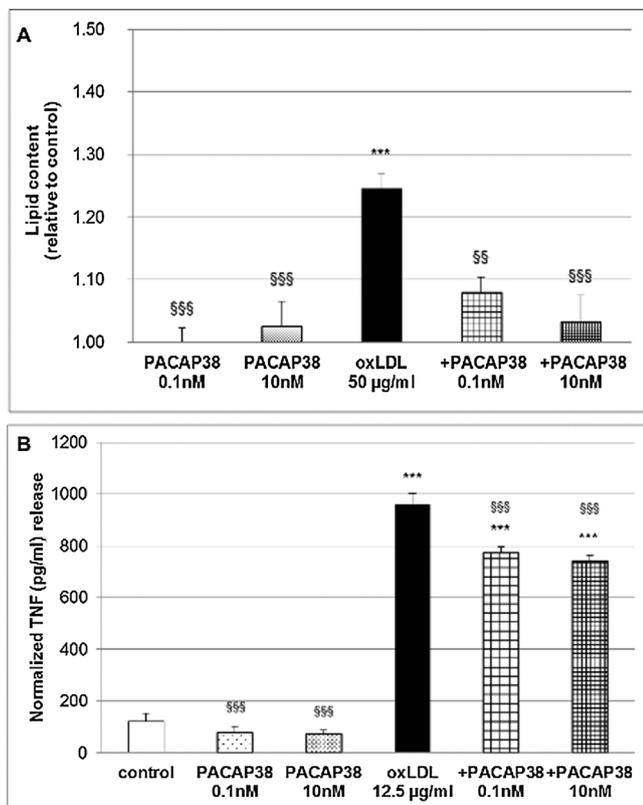
Fig. 1. Effect of exogenous pituitary adenylate cyclase activating polypeptide-38 (PACAP38) on lipid storage (A) and TNF (B) release in cultured PMA-differentiated THP-1 MΦ, treated with 0.1 nM or 10 nM PACAP38 and together with oxLDL or left untreated (control) for 24 h. The intracellular lipid level was determined by Oil Red O staining and TNF release by ELISA. One Way Analysis of Variance (ANOVA). Bars represent means + SEM of 3–5 experiments. ***$P < 0.001$ vs. control; §§$P < 0.01$, §§§$P < 0.001$ vs. oxLDL.

3.2. PACAP inhibits oxLDL-induced TNF release of human MΦ in vitro

Stimulation of PMA-differentiated human THP-1 MΦ with 12.5 μg/ml oxLDL revealed a 6.9-fold increase in TNF release as compared to the negative control (Fig. 1B). However, incubation of human THP-1 MΦ with 12.5 μg/ml oxLDL and additional treatment with 0.1 nM or 10 nM recombinant PACAP38 inhibited the oxLDL-induced TNF release by 19.3% ($p < 0.001$) and 22.5% ($p < 0.001$), respecively (Fig. 1B). Treatment of unstimulated human THP-1 MΦ with PACAP38 alone exhibited no significant effect on TNF release as compared to the negative control (Fig. 1B).

3.3. PACAP deficiency affects the body weight

After 30 weeks SC, PACAP$^{-/-}$/ApoE$^{-/-}$ mice revealed a 12.7% ($p < 0.05$) lower body weight than ApoE$^{-/-}$ mice (Table 3). However, after CED, PACAP$^{-/-}$/ApoE$^{-/-}$ mice showed a 13.3% ($p < 0.05$) higher body weight than ApoE$^{-/-}$ mice (Table 3). After CED, PACAP$^{-/-}$/ApoE$^{-/-}$ mice were 25.6% ($p < 0.01$) heavier than the mice which received SC (Table 3). These differences observed in body weight are not related to the size of the mice as indicated by the similar tibia lengths among the different experimental groups (Table 3).

3.4. PACAP deficiency increases the development of atherosclerotic lesions in the brachiocephalic trunk after SC but not after CED

A histopathologic hallmark of atherosclerotic disease is the abnormal narrowing of blood vessels caused by the development of lesions that occlude the vascular lumen. In this context, we found that

Table 3
Effect of PACAP deficiency on body weight, tibia length, plasma cholesterol and triglyceride levels.

	ApoE$^{-/-}$ (n)	PACAP$^{-/-}$/ApoE$^{-/-}$ (n)	p <
Body weight (g)			
30 wks SC	33.2 ± 1.0 (13)	29.0 ± 0.9 (7)	0.05
10 wks SC + 20 wks CED	33.8 ± 0.8 (16)	39.0 ± 1.9 (16)	0.05
p < vs 30 wks SC	N.S.	0.01	
Tibia length (mm)			
30 wks SC	19.3 ± 0.3 (12)	18.3 ± 0.7 (7)	N.S.
10 wks SC + 20 wks CED	19.4 ± 0.5 (16)	19.6 ± 0.2 (16)	N.S.
p < vs 30 wks SC	N.S.	N.S.	
Cholesterol (mg/dl)			
30 wks SC	554.0 ± 43 (13)	472.1 ± 30 (12)	N.S.
10 wks SC + 20 wks CED	1019.7 ± 133 (11)	893.3 ± 86 (16)	N.S.
p < vs 30 wks SC	0.01	0.001	
Triglyceride (mg/dl)			
30 wks SC	83.7 ± 13 (9)	105.1 ± 19 (7)	N.S.
10 wks SC + 20 wks CED	95.8 ± 10 (10)	140.3 ± 9 (15)	0.001
p < vs 30 wks SC	N.S.	N.S.	

ApoE indicates apolipoprotein E; CED, cholesterol-enriched diet; SC, standard chow; PACAP, pituitary adenylate cyclase activating polypeptide; wks, weeks.

PACAP$^{-/-}$/ApoE$^{-/-}$ mice showed a 9.8-fold ($p < 0.001$) increase in maximal lumen stenosis compared to the ApoE$^{-/-}$ mice after 30 weeks SC (Fig. 2A–E). However, after CED no difference in maximal lumen stenosis was found between PACAP$^{-/-}$/ApoE$^{-/-}$ and ApoE$^{-/-}$ mice (Fig. 2A).

3.5. PACAP deficiency does not affect plasma cholesterol concentrations

To consider the possibility that the observed effects of PACAP deficiency on atherosclerotic vascular remodelling are related to changes in serum lipid signatures, plasma concentrations of total cholesterol and triglycerides were determined. Neither after SC nor after CED, were significant differences in total plasma cholesterol levels were observed between PACAP$^{-/-}$/ApoE$^{-/-}$ and ApoE$^{-/-}$ mice (Table 3). In contrast, the comparison of CED vs. SC showed significantly increased plasma cholesterol concentrations of 1.8-fold ($p < 0.01$) and 1.9-fold ($p < 0.001$) in ApoE$^{-/-}$ and PACAP$^{-/-}$/ApoE$^{-/-}$ mice, respectively. After CED, plasma triglyceride levels were increased 1.5-fold ($p < 0.001$) in PACAP$^{-/-}$/ApoE$^{-/-}$ compared to ApoE$^{-/-}$ mice, whereas plasma triglyceride levels remained unchanged after SC (Table 3).

3.6. PACAP deficiency increases the expression of pro-inflammatory cytokines TNF and IL-1β

To test the hypothesis that inflammatory processes, occurring in atherosclerotic lesions, are modulated by PACAP deficiency, inflammatory markers were analysed by immunohistochemistry as depicted in Fig. 3. In atherosclerotic lesions of PACAP$^{-/-}$/ApoE$^{-/-}$ mice, the percentage of immunoreactive areas of TNF (62.7%, $p < 0.05$) and interleukin 1 beta (IL-1β; 74.7%, $p < 0.05$) are increased after 30 weeks of SC in comparison with ApoE$^{-/-}$ mice (Fig. 3A and B). In PACAP$^{-/-}$/ApoE$^{-/-}$ mice, the percentage of TNF immunoreactive areas in atherosclerotic lesions was 55.4% ($p < 0.05$) lower after 20 weeks CED than after 30 wks SC (Fig. 3A). In contrast, the percentage of interleukin-6 (IL-6) and cyclooxygenase-2 (COX-2) immunoreactive areas in atherosclerotic lesions were not affected by PACAP deficiency, neither under SC nor under CED (Fig. 3D).
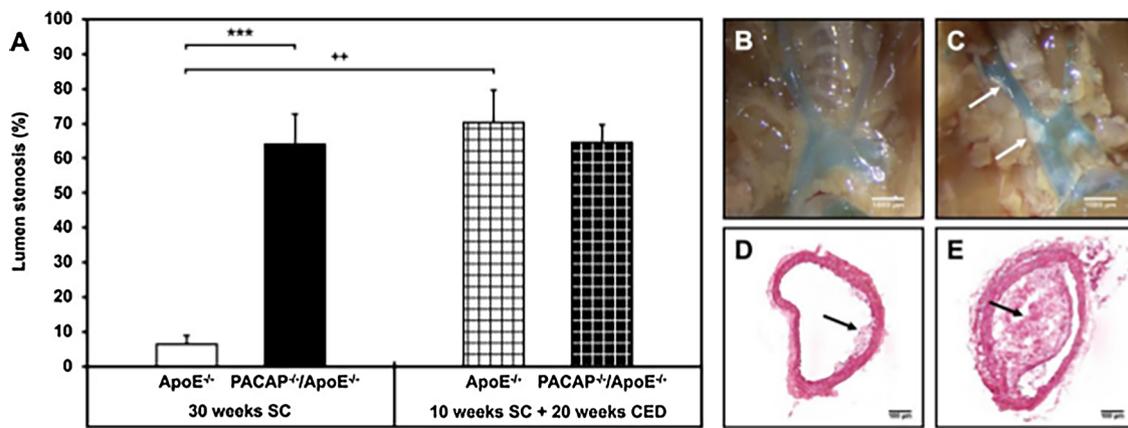
Fig. 2. Effect of PACAP deficiency on lumen stenosis in brachiocephalic trunk (BT). Maximal lumen stenosis observed in ApoE$^{-/-}$ and PACAP$^{-/-}$/ApoE$^{-/-}$ mice after 30 weeks SC or 10 weeks SC and afterwards 20 weeks CED (A). Representative images of the BT in situ of ApoE$^{-/-}$ (B) and PACAP$^{-/-}$/ApoE$^{-/-}$ mice (C) after 30 weeks SC, atherosclerotic lesions are indicated with white arrows. Representative cross-sections after hematoxylin and eosin staining in ApoE$^{-/-}$ (D) and PACAP$^{-/-}$/ApoE$^{-/-}$ (E) mice, black arrows indicate atherosclerotic plaques. Data given as mean + SEM (n = 5-8). 2-tailed Student's *t*-test or Mann–Whitney *U* test were performed as appropriate. Comparison within 30 weeks SC: PACAP$^{-/-}$/ApoE$^{-/-}$ vs. ApoE$^{-/-}$, ***$P < 0.001$. Comparison within ApoE$^{-/-}$: 30 weeks SC vs. 10 weeks SC + 20 weeks CED, $^{++}P < 0.01$. SC indicates standard chow; CED, cholesterol-enriched diet. Scale bar, B, C = 1000 μm; D, E = 100 μm.

3.7. PACAP deficiency inhibits cell proliferation in atherosclerotic plaques of ApoE$^{-/-}$ mice after SC

After 30 weeks SC, the percentage of Ki67 immunoreactive cell nuclei in atherosclerotic plaques of PACAP$^{-/-}$/ApoE$^{-/-}$ mice has been found to be decreased by -26.9% (p < 0.05) as compared to ApoE$^{-/-}$ mice (Fig. 4A) indicating reduction of proliferation due to PACAP deficiency. After CED, the percentage of Ki67 immunoreactive cell nuclei in atherosclerotic lesions of ApoE$^{-/-}$ mice has been found to be -37.5% (p < 0.01) lower than in ApoE$^{-/-}$ mice after SC (Fig. 4A) indicating that CED might exert anti-proliferative effects in ApoE$^{-/-}$ mice.

3.8. PACAP deficiency increases expression of autophagy-, apoptosis- and necroptosis-relevant proteins in atherosclerotic plaques after SC

After 30 weeks SC, we found a 87.0% (p < 0.05) increase of active caspase-3 immunoreactivity in atherosclerotic plaques of PACAP$^{-/-}$/ApoE$^{-/-}$ mice in comparison with ApoE$^{-/-}$ mice (Fig. 4B). After 30 weeks SC, the immunoreactive areas of autophagy (ATG5) and necroptosis (RIP3) relevant proteins in atherosclerotic lesions of PACAP$^{-/-}$/ApoE$^{-/-}$ mice revealed an increase of 90.2% (p < 0.01) and 97.2% (p < 0.01), respectively, as compared to ApoE$^{-/-}$ mice (Fig. 4C and 4D). After 30 weeks of CED, however, the immunoreactive areas of ATG5 and RIP3 in atherosclerotic plaques of PACAP$^{-/-}$/ApoE$^{-/-}$ mice were 60.6% (p < 0.01) and 60.1% lower than after SC, respectively (Fig. 4C and 4D).

3.9. PACAP deficiency decreases the cell density and increases collagen deposition in atherosclerotic lesions after SC

We next investigated the cellularity of the atherosclerotic lesions (Fig. 5A). We found a 49.5% reduction (p < 0.05) of the cell density in atherosclerotic lesions of PACAP$^{-/-}$/ApoE$^{-/-}$ mice after 30 weeks SC when compared with ApoE$^{-/-}$ mice (Fig. 5A). However, after CED, the cell density in atherosclerotic plaques of ApoE$^{-/-}$ mice was 45.0% (p < 0.05) lower than in ApoE$^{-/-}$ mice after 30 weeks SC (Fig. 5A). After 30 weeks SC, the immunoreactive area of MΦ (CD68$^+$) in atherosclerotic plaques of PACAP$^{-/-}$/ApoE$^{-/-}$ mice was 66.4% (p < 0.05) lower than in ApoE$^{-/-}$ mice (Fig. 5B). Moreover, the immunoreactive area of MΦ in atherosclerotic lesions of ApoE$^{-/-}$ mice, was 76.7% (p < 0.05) lower after CED than that after SC (Fig. 5B). Furthermore, after 30 weeks SC, we found a 93.2% increase (p < 0.05)

of the collagen content in plaques of PACAP$^{-/-}$/ApoE$^{-/-}$ mice when compared to ApoE$^{-/-}$ mice (Fig. 5C). However, after CED, the amount of collagen in atherosclerotic plaques of PACAP$^{-/-}$/ApoE$^{-/-}$ mice was 86.3% (p < 0.01) higher than that in ApoE$^{-/-}$ mice (Fig. 5C). Additionally, after CED, in atherosclerotic plaques of PACAP$^{-/-}$/ApoE$^{-/-}$ mice the amount of collagen was significantly 61.0% (p < 0.05) higher than in atherosclerotic lesions of PACAP$^{-/-}$/ApoE$^{-/-}$ after SC (Fig. 5C). Yet, the amount of vascular SMC in the atherosclerotic plaques is neither affected by PACAP deficiency nor by different feeding conditions (Fig. 5D).

4. Discussion

The presence of PACAP and its receptor PAC1 in cardiac tissue and blood vessels (Chang, 1997; Gasz et al., 2006; Merriam et al., 2013) implies the possibility that PACAP signaling may play a yet unrecognized and potentially crucial role in atherogenesis. Indeed, we provide in our present study strong evidence for this working hypothesis through both mechanistic experiments in cell culture and *in vivo*. Related to this topic, other authors using mouse models of myocarditis and atherosclerosis have most recently demonstrated that VIP, a neuropeptide closely related to PACAP, attenuated heart hypertrophy, myocardial inflammation and injury as well as ameliorated atherosclerotic plaque formation leading to the conclusion that VIP protects from inflammatory cardiovascular diseases (Benitez et al., 2018).

We found that treatment of PMA-differentiated human THP-1 MΦs with oxLDL induced an increase in lipid internalization and TNF release, whereby both effects of oxLDL were shown to be significantly attenuated by treatment with PACAP38. Thus, we demonstrate for the first time, that PACAP38 is able to inhibit the internalization of cholesterol and TNF release by macrophages. These results are in line with and extend most recent data of others, showing that VIP regulates cholesterol efflux in macrophages and inhibits foam cell formation in atherosclerotic plaques (Benitez et al., 2018); thus, these common effects of VIP and PACAP are likely to be mediated by VPAC1-R and/or VPAC2-R. Unlike VIP, PACAP could in addition interact with PAC1-R (Moody et al., 2011). Our results suggest that PACAP, whether generated at the sight of MΦ inflammation or provided pharmacologically, has anti-atherosclerotic properties which might be associated with an anti-inflammatory effect. PACAP has been shown to significantly increase the production of anti-atherosclerotic substances and to inhibit the production of lipid peroxides by EC and SMC in culture under hyperlipidemic circumstances, consistent with the cytoprotective, anti-
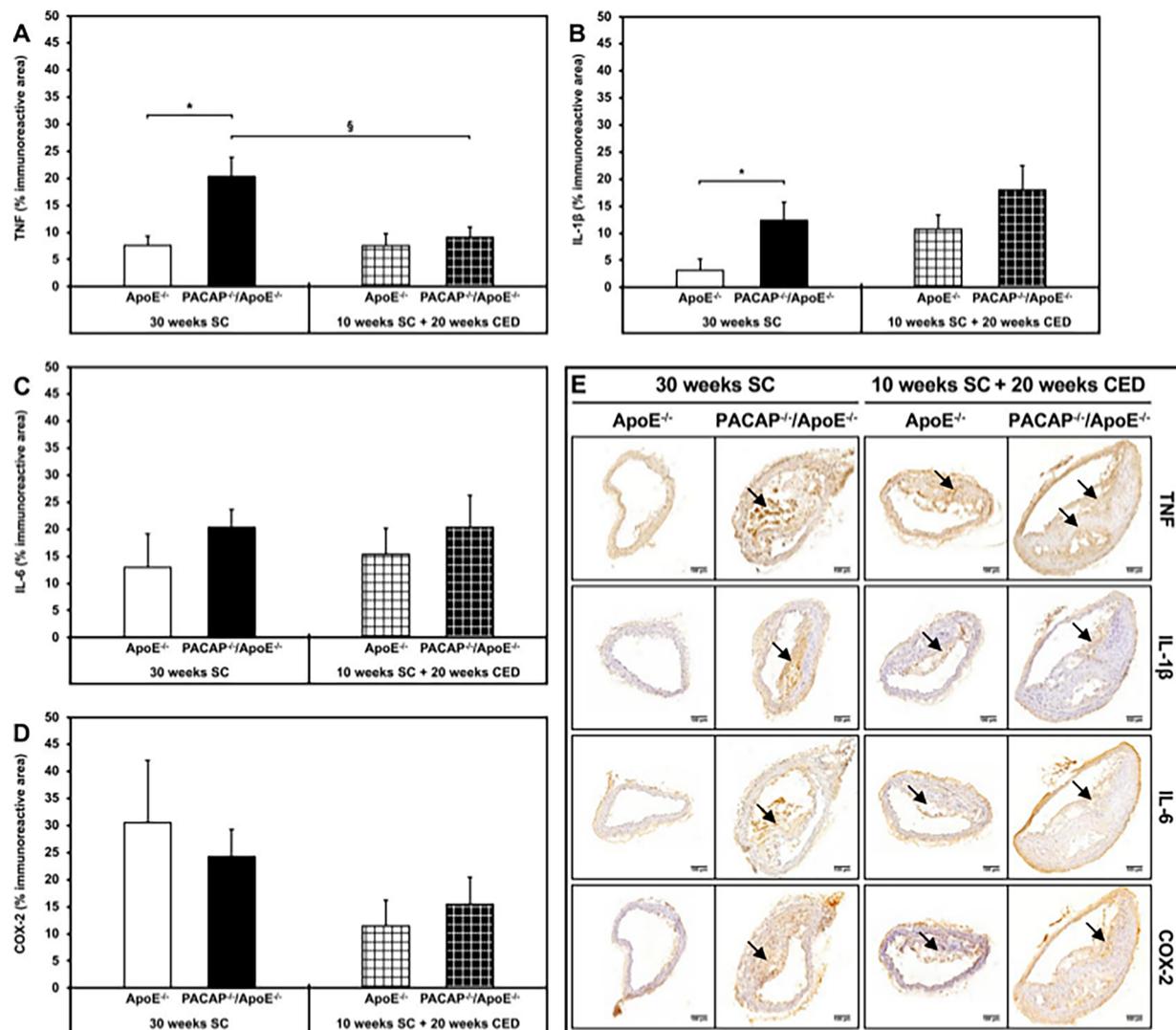
Fig. 3. Effect of PACAP deficiency on immune signature of atherosclerotic plaques in the brachiocephalic trunk (BT). Immunohistomorphometric analyses of atherosclerotic lesions observed in ApoE$^{-/-}$ and PACAP$^{-/-}$/ApoE$^{-/-}$ mice after 30 weeks SC or 10 weeks SC and afterwards 20 weeks CED. Analysis of inflammation markers TNF (A), IL-1β (B), IL-6 (C) and cyclooxygenase (COX)-2 (D) on cryo cross-sections of the BT as well as representative photomicrographs (E) are shown. Data given as mean + SEM (n = 4-6). 2-tailed Student's t-test or Mann–Whitney U test were performed as appropriate. Comparisons within 30 weeks SC: PACAP$^{-/-}$/ApoE$^{-/-}$ vs. ApoE$^{-/-}$, *P < 0.05. Comparisons within PACAP$^{-/-}$/ApoE$^{-/-}$: 30 weeks SC vs. 10 weeks SC + 20 weeks CED, $^{§}P$ < 0.05. SC indicates standard chow; CED, cholesterol-enriched diet. Black arrows indicate positive reaction. Scale bar = 100 μm.

inflammatory and anti-atherosclerotic effects of PACAP demonstrated here (Diané et al., 2014; Chang, 1997). Recent findings showing that PACAP exerts a cytoprotective effect on EC exposed to TNF (Bian et al., 2017) lend support to a general anti-inflammatory role of PACAP in vascular diseases.

To demonstrate that PACAP has effects on plaque development as well as on generally accepted inflammatory and plaque stability parameters *in vivo*, a standard atherosclerosis ApoE$^{-/-}$ mouse model has been used in combination with PACAP gene deficiency. The principal new finding of this study was that PACAP deficiency in ApoE$^{-/-}$ mice promotes atherosclerotic plaque development under SC (30 weeks). However, CED does not enhance atherosclerosis progression in PACAP$^{-/-}$/ApoE$^{-/-}$ mice, neither in comparison with ApoE$^{-/-}$ (after 20 weeks CED) nor with PACAP$^{-/-}$/ApoE$^{-/-}$ mice (after SC). Interestingly, the plasma cholesterol levels were not different between PACAP$^{-/-}$/ApoE$^{-/-}$ and ApoE$^{-/-}$ mice, neither after (i) SC nor (ii) CED, whereas the cholesterol levels within the respective genotype were significantly higher after CED than after SC. An explanation of the mentioned unexpected lack of difference in the percentage of lumen stenosis between PACAP$^{-/-}$/ApoE$^{-/-}$ compared to ApoE$^{-/-}$ mice

after CED may be due to the lack of difference between the amount of TNF, IL1-β, Ki67, caspase-3, ATG5 and RIP3 immunoreactive areas in atherosclerotic plaques of the two mouse genotypes after CED indicating that these factors may be crucially involved in regulation of the development and progression of atherosclerotic plaques.

Our results provide the first evidence that endogenous PACAP plays a direct role in the development of atherosclerosis. However, because after CED there were no significant differences in maximal lumen stenosis between PACAP$^{-/-}$/ApoE$^{-/-}$ and ApoE$^{-/-}$ mice, it is worth noting that the morphological parameters of almost all immunohistologically investigated parameters (e.g. proliferation, apoptosis, autophagy, necroptosis, cell density, SMC α-actin, macrophages) of atherosclerotic plaques were not different between PACAP$^{-/-}$/ApoE$^{-/-}$ and ApoE$^{-/-}$ mice after CED.

In relation to this morphological aspect, our findings that PACAP deficiency results in increased proliferation of cells in the vascular wall correspond to previous observations that the proliferation of gut myocytes and aortic SMCs is inhibited by PACAP (Van Assche et al., 1999; Oiso et al., 1993). Consistently, we found in atherosclerotic plaques of PACAP$^{-/-}$/ApoE$^{-/-}$ mice a decrease in the percentage of nuclei
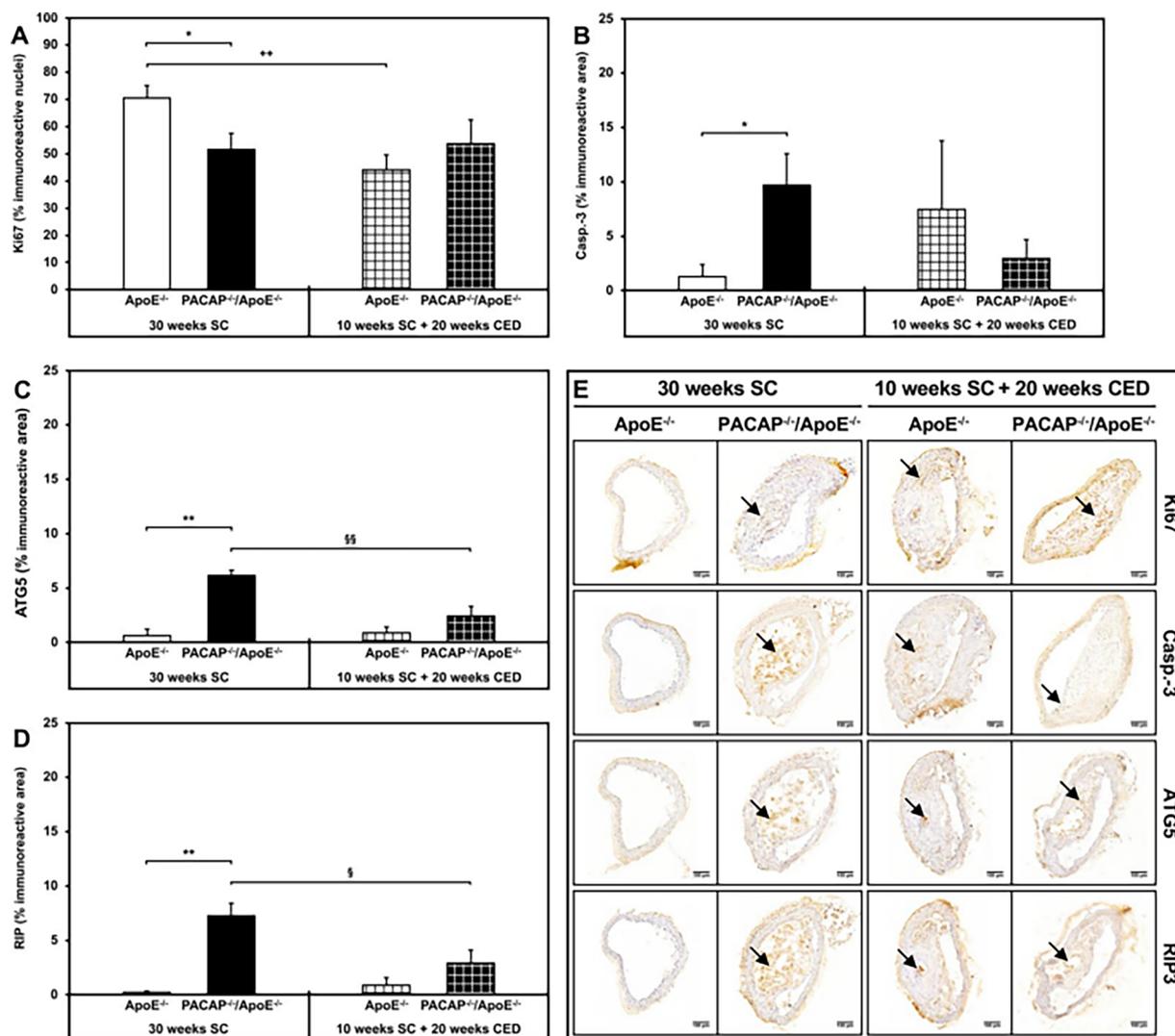
Fig. 4. Effect of PACAP deficiency on atherosclerotic plaque remodeling in the brachiocephalic trunk (BT). Immunohistomorphometric analyses of atherosclerotic lesions observed in ApoE$^{-/-}$ and PACAP$^{-/-}$/ApoE$^{-/-}$ mice after 30 weeks SC or 10 weeks SC and afterwards 20 weeks CED. Analysis of Ki67 (A), Caspase-3 (B), ATG5 (C) and RIP3 (D) on cryo cross-sections of the BT as well as representative photomicrographs (E) are shown. Data given as mean + SEM (n = 5-7). 2-tailed Student's *t*-test or Mann–Whitney *U* test were performed as appropriate. Comparisons within 30 weeks SC: PACAP$^{-/-}$/ApoE$^{-/-}$ vs. ApoE$^{-/-}$, **$P < 0.01$, *$P < 0.05$. Comparisons within ApoE$^{-/-}$: 30 weeks SC vs. 10 weeks SC + 20 weeks CED, $^{++}P < 0.01$. Comparisons within PACAP$^{-/-}$/ApoE$^{-/-}$: 30 weeks SC vs. 10 weeks SC + 20 weeks CED, $^{§§}P < 0.01$, $^{§}P < 0.05$. SC indicates standard chow; CED, cholesterol-enriched diet. Black arrows indicate positive reaction. Scale bar = 100 μm.

immunopositive for the proliferation marker Ki67 in conjunction with a significant increase of apoptotic cells. In this regard, we show an increase of ATG5 (autophagy) expression in PACAP$^{-/-}$/ApoE$^{-/-}$ mice compared with the ApoE$^{-/-}$ mice after SC (30 weeks). Additionally, we observed in most of the atherosclerotic lesions of PACAP$^{-/-}$/ApoE$^{-/-}$ mice characteristic structures of an unstable plaque including necrotic cores. Our data indicate that PACAP obviously is only able to mitigate plaque development up to a distinct plasma cholesterol level, e.g. about 500 mg/dl in mice (as suggested according to our experiments). Doubling of these cholesterol concentrations, i.e. up to about 1000 mg/dl seems to overwhelm the protective effects of PACAP. Alternatively, CED may not potentiate the pro-atherogenic effects under conditions of PACAP deficiency. In this context, it has recently been noted that high-fat and calorie rich-diets trigger an innate immune inflammatory response similar to that of pathogens, resulting in a systemic, long-term pro-inflammatory effect (Christ et al., 2018). Given the causal relationship between high fat diet, inflammation and atherosclerosis development, the enhanced pro-inflammatory as well as pro-atherogenic effect of CED may be sufficiently robust so that the pro-

atherogenic effect of PACAP-deficiency observed under SC is obscured under CED with maximal atherosclerotic lesioning occurring despite the presence of PACAP.

In agreement with a previous report that PACAP influences inflammatory processes by modulating the function of various cells resulting in anti-inflammatory and neuroprotective effects (Waschek, 2013), we report here, that PACAP deficiency in ApoE$^{-/-}$ mice increased the expression of the pro-inflammatory cytokines TNF and IL-1β coincidently with increased lumen stenosis under SC. We have shown that in the absence of endogenous PACAP the ApoE knockout mice develop atherosclerosis without Western -type diet whereas the Western type diet-induced aggravation of atherosclerosis is unaffected by the lack of PACAP in the ApoE knockout mice. We conclude that not enough endogenous PACAP is produced to counteract Western-type diet-induced aggravation of atherogenesis. Thus, our experiments demonstrate the unexpected finding that PACAP-deficient ApoE knockout mice develop an atherogenic phenotype without Western-type diet. Therefore, we propose that these PACAP/ApoE double knockout mice represent a new genetic model of atherogenesis without Western-type
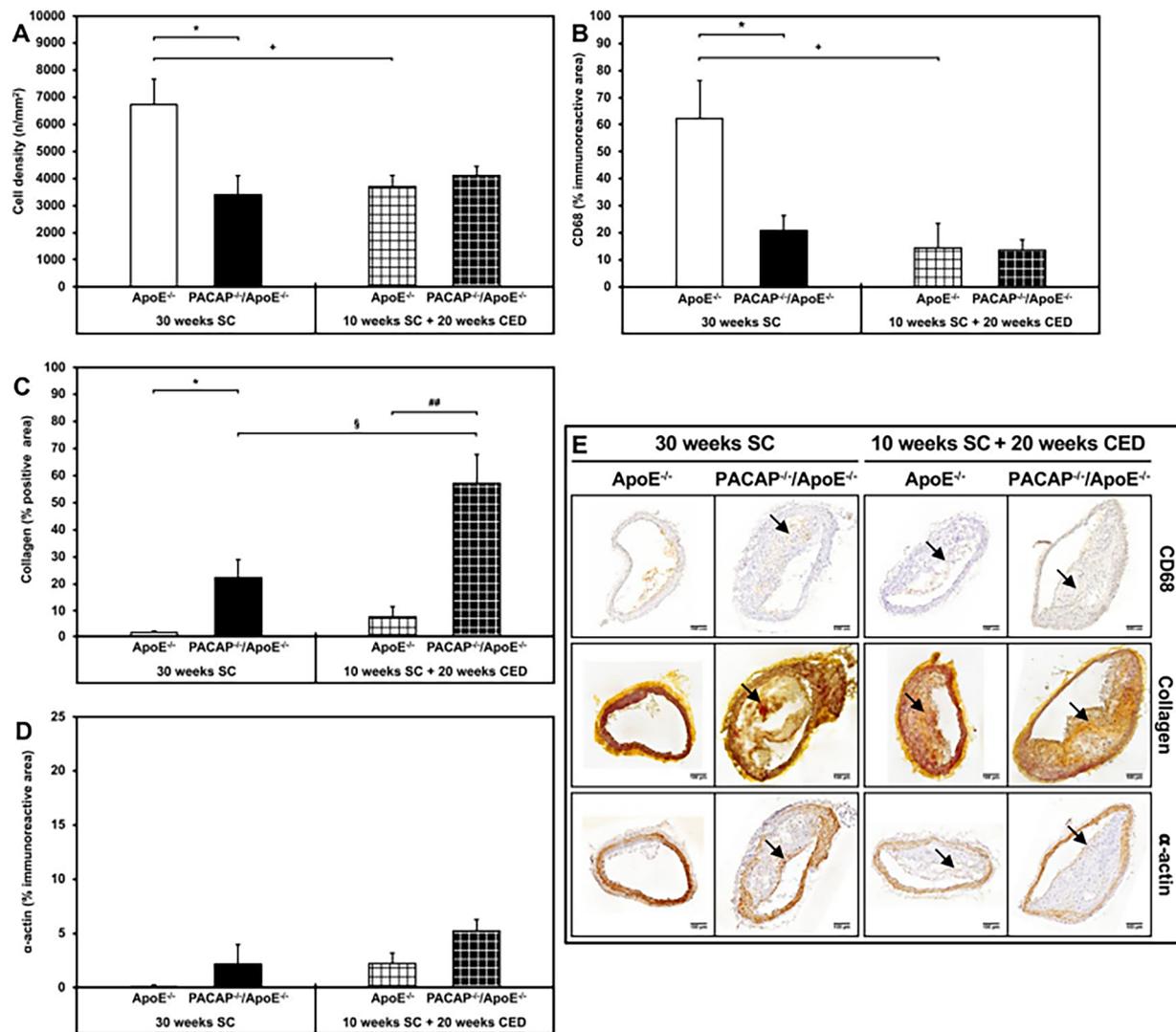
Fig. 5. Effect of PACAP deficiency on atherosclerotic plaque morphology in the brachiocephalic trunk (BT). Immunohistomorphometric analyses of atherosclerotic lesions observed in ApoE$^{-/-}$ and PACAP$^{-/-}$/ApoE$^{-/-}$ mice after 30 weeks SC or 10 weeks SC and afterwards 20 weeks CED. Analysis of cell density (A), CD68 (B), collagen (C) and α-actin (D) on cryo cross-sections of the BT as well as representative photomicrographs (E) are shown. Data given as mean + SEM (n = 4–6). 2-tailed Student's *t*-test or Mann–Whitney *U* test were performed as appropriate. Comparisons within 30 weeks SC: PACAP$^{-/-}$/ApoE$^{-/-}$ vs. ApoE$^{-/-}$, *P < 0.05. Comparisons within 10 weeks SC + 20 weeks CED: PACAP$^{-/-}$/ApoE$^{-/-}$ vs. ApoE$^{-/-}$, ##P < 0.01. Comparisons within ApoE$^{-/-}$: 30 weeks SC vs. 10 weeks SC + 20 weeks CED, +P < 0.05. Comparisons within PACAP$^{-/-}$/ApoE$^{-/-}$: 30 weeks SC vs. 10 weeks SC + 20 weeks CED, §P < 0.05. SC indicates standard chow; CED, cholesterol-enriched diet. Black arrows indicate positive reaction. Scale bar = 100 μm.

diet.

Taken together, our present data demonstrate that PACAP deficiency in ApoE$^{-/-}$ mice aggravates the development and progression of atherosclerotic plaques up to a distinct plasma cholesterol level or lumen stenosis. ThusPACAP is suggested to act as an endogenous atheroprotectant. The postulated atheroprotective effects of PACAP may involve inhibition of proatherogenic increases of TNF-α, IL-1β, autophagy (ATG5), apoptosis (active caspase-3), necroptosis (RIP3) and fibrosis (collagen). Therefore, stable PACAP agonists may have translational potential as a novel class of atheroprotective therapeutics. However, it remains to be determined, which of the three PACAP receptors (VPAC1, VPAC2, PAC1) alone or in combination mediates the atheroprotection (Arimura and Shioda, 2018).

Conflict of interest

The authors declare no potential conflicts of interest.

References

Arimura, A., Shioda, S., 2018. Pituitary adenylate cyclase activating polypeptide (PACAP) and its receptors: neuroendocrine and endocrine interaction. Front. Neuroendocrinol. 16, 53–88. https://doi.org/10.1006/frne.1003.

Benitez, R., Delgado-Maroto, V., Caro, M., Forte-Lago, I., Duran-Prado, M., O'Valle, F., Lichtman, A., Gonzalez-Rey, E., Delgado, M., 2018. Vasoactive intestinal peptide ameliorates acute myocarditis and atherosclerosis by regulating inflammatory and autoimmune responses. J. Immunol. 200 (11), 3697–3710. https://doi.org/10.4049/jimmunol.1800122. (Epub 2018 April 18).

Bentzon, J.F., Otsuka, F., Virmani, R., Falk, E., 2014. Mechanisms of plaque formation and rupture. Circ. Res. 114 (12), 1852–1866. https://doi.org/10.1161/CIRCRESAHA.114.302721.

Bian, N., Du, G., Ip, M.F., Ding, J., Chang, Q., Li, Z., 2017. Pituitary adenylate cyclase-activating polypeptide attenuates tumor necrosis factor-α-induced apoptosis in endothelial colony-forming cells. Biomed. Rep. 7 (1), 11–16. https://doi.org/10.3892/br.2017.917.

Chang, Q., 1997. Experimental study of the effects of pituitary adenylate cyclase-activating polypeptide (PACAP) and its mechanism on the vascular cell components—the possible relationship between PACAP and atherosclerosis. Sheng Li Ke Xue Jin Zhan 28 (2), 132–135.

Christ, A., Günther, P., Lauterbach, M.A.R., Duewell, P., Biswas, D., Pelka, K., Scholz, C.J., Oosting, M., Haendler, K., Baßler, K., Klee, K., Schulte-Schrepping, J., Ulas, T., Moorlag, S.J.C.F.M., Kumar, V., Park, M.H., Joosten, L.A.B., Groh, L.A., Riksen, N.P., Espevik, T., Schlitzer, A., Li, Y., Fitzgerald, M.L., Netea, M.G., Schultze, J.L., Latz, E., 2018. Western diet triggers NLRP3-dependent innate immune reprogramming. Cell 172 (1–2), https://doi.org/10.1016/j.cell.2017.12.013. 162–175.e14.

Delgado, M., Pozo, D., Martinez, C., Leceta, J., Calvo, J.R., Ganea, D., Gomariz, R.P., 1999. Vasoactive intestinal peptide and pituitary adenylate cyclase-activating polypeptide inhibit endotoxin-induced TNF-alpha production by macrophages: in vitro and in vivo studies. J. Immunol. 162 (4), 2358–2367.

Diané, A., Payne, G.W., Gray, S.L., 2014. Multifaces of pituitary adenylate cyclase-activating polypeptide (PACAP): from neuroprotection and energy homeostasis to respiratory and cardiovascular systems. J. Metab. Syndr. 3, 4. https://doi.org/10.4172/2167-0943.1000162.

Galle, J., Wanner, C., 1998. Oxidized LDL and Lp(a) preparation, modification, and analysis. Methods Mol. Biol. 108, 119–130. https://doi.org/10.1385/0-89603-472-0:119.

Ganea, D., Delgado, M., 2001. Neuropeptides as modulators of macrophage functions: regulation of cytokine production and antigen presentation by VIP and PACAP. Arch. Immunol. Ther. Exp. (Warsz) 49 (2), 101–110.

Gasz, B., Rácz, B., Roth, E., Borsiczky, B., Ferencz, A., Tamás, A., Cserepes, B., Lubics, A., Gallyas Jr., F., Tóth, G., Lengvári, I., Reglodi, D., 2006. Pituitary adenylate cyclase activating polypeptide protects cardiomyocytes against oxidative stress-induced apoptosis. Peptides 27, 87–94. https://doi.org/10.1016/j.peptides.2005.06.022.

Hamelink, C., Tjurmina, O., Damadzic, R., Young, W.S., Weihe, E., Lee, H.W., Eiden, L.E., 2002. Pituitary adenylate cyclase-activating polypeptide is a sympathoadrenal neurotransmitter involved in catecholamine regulation and glucohomeostasis. Proc. Natl. Acad. Sci. U. S. A. 99 (1), 461–466. https://doi.org/10.1073/pnas.012608999.

Harmar, A.J., Arimura, A., Gozes, I., Journot, L., Laburthe, M., Pisegna, J.R., Rawlings, S.R., Robberecht, P., Said, S.I., Sreedharan, S.P., Wank, S.A., Waschek, J.A., 1998. International Union of Pharmacology. XVIII. Nomenclature of receptors for vasoactive intestinal peptide and pituitary adenylate cyclase-activating polypeptide. Pharmacol. Rev. 50 (2), 265–270.

Holgert, H., Holmberg, K., Hannibal, J., Fahrenkrug, J., Brimijoin, S., Hartman, B.K., Hökfelt, T., 1996. PACAP in the adrenal gland—relationship with choline acetyltransferase, enkephalin and chromaffin cells and effects of immunological sympathectomy. Neuroreport 8 (1), 297–301.

Holighaus, Y., Mustafa, T., Eiden, L.E., 2011. PAC1hop, null and hip receptors mediate differential signaling through cyclic AMP and calcium leading to splice variant-specific gene induction in neural cells. Peptides 32 (8), 1647–1655. https://doi.org/10.1016/J.PEPTIDES.2011.06.004. (Elsevier).

Kinscherf, R., Deigner, H.P., Usinger, C., Pill, J., Wagner, M., Kamencic, H., Hou, D.,

Chen, M., Schmiedt, W., Schrader, M., Kovacs, G., Kato, K., Metz, J., 1997. Induction of mitochondrial manganese superoxide dismutase in macrophages by oxidized LDL: its relevance in atherosclerosis of humans and heritable hyperlipidemic rabbits. FASEB J. 11 (14), 1317–1328.

Libby, P., Ridker, P.M., Hansson, G.K., 2011. Progress and challenges in translating the biology of atherosclerosis. Nature 473 (7347), 317–325. https://doi.org/10.1038/nature10146.

May, V., Parsons, R.L.G., 2017. Protein-coupled receptor endosomal signaling and regulation of neuronal excitability and stress responses: signaling options and lessons from the PAC1 receptor. J. Cell. Physiol. 232 (4), 698–706. https://doi.org/10.1002/jcp.25615.

Merriam, L.A., Baran, C.N., Girard, B.M., Hardwick, J.C., May, V., Parsons, R.L., 2013. Pituitary adenylate cyclase 1 receptor internalization and endosomal signaling mediate the pituitary adenylate cyclase activating polypeptideinduced increase in guinea pig cardiac neuron excitability. J. Neurosci. 33, 4614–4622. https://doi.org/10.1523/JNEUROSCI.4999-12.2013.

Miyata, A., Arimura, A., Dahl, R.R., Minamino, N., Uehara, A., Jiang, L., Culler, M.D., Coy, D.H., 1989. Isolation of a novel 38 residue-hypothalamic polypeptide which stimulates adenylate cyclase in pituitary cells. Biochem. Biophys. Res. Commun. 164 (1), 567–574.

Moody, T.W., Ito, T., Osefo, N., Jensen, R.T., 2011. VIP and PACAP: recent insights into their functions/roles in physiology and disease from molecular and genetic studies. Curr. Opin. Endocrinol. Diabetes Obes. 18 (1), 61–67. https://doi.org/10.1097/MED.0b013e328342568a.

Moore, K.J., Tabas, I., 2011. Macrophages in the pathogenesis of atherosclerosis. Cell 145 (3), 341–355. https://doi.org/10.1016/j.cell.2011.04.005.

Moore, K.J., Sheedy, F.J., Fisher, E.A., 2013. Macrophages in atherosclerosis: a dynamic balance. Nat. Rev. Immunol. 13 (10), 709–721. https://doi.org/10.1038/nri3520.

Nandha, K.A., Benito-Orfila, M.A., Smith, D.M., Ghatei, M.A., Bloom, S.R., 1991. Action of pituitary adenylate cyclase-activating polypeptide andvasoactive intestinal polypeptide on the rat vascular system: effects on blood pressure and receptor binding. J. Endocrinol. 129, 69–73.

Oiso, Y., Kotoyori, J., Murase, T., Ito, Y., Kozawa, O., 1993. Effect of pituitary adenylate cyclase activating polypeptide on vasopressin-induced proliferation of aortic smooth muscle cells: comparison with vasoactive intestinal polypeptide. Biochem. Cell. Biol. 71 (3–4), 156–161 (11038706).

Romeis, B., 1989. Trichromfärbung nach Wallart und Houette. In: In: Böck, P. (Ed.), Mikroskopische Technik 989. Urban & Schwarzenberg, München-Wien-Baltimore, pp. 599.

Rosenfeld, M.E., Polinsky, P., Virmani, R., Kauser, K., Rubanyi, G., Schwartz, S.M., 2000. Advanced atherosclerotic lesions in the innominate artery of the ApoE knockout mouse. Arterioscler. Thromb. Vasc. Biol. 20 (12), 2587–2592.

Steinbrecher, U.P., 1987. Oxidation of human low density lipoprotein results in derivatization of lysine residues of apolipoprotein B by lipid peroxide decomposition products. J. Biol. Chem. 262 (8), 3603–3608.

Stroth, N., Holighaus, Y., Ait-Ali, D., Eiden, L.E., 2011. PACAP: A master regulator of neuroendocrine stress circuits and the cellular stress response. Ann. N. Y. Acad. Sci. 1220 (1), 49–59. https://doi.org/10.1111/j.1749-6632.2011.05904.x.

Tabas, I., Williams, K.J., Boren, J., 2007. Subendothelial lipoprotein retention as the initiating process in atherosclerosis: update and therapeutic implications. Circulation 116 (16), 1832–1844. https://doi.org/10.1161/CIRCULATIONAHA.106.676890.

Tsuchiya, S., Yamabe, M., Yamaguchi, Y., Kobayashi, Y., Konno, T., Tada, K., 1980. Establishment and characterization of a human acute monocytic leukemia cell line (THP-1). Int. J. Cancer 26 (2), 171–176.

Van Assche, G., Depoortere, I., de Vos, R., Geboes, K., Janssens, J.J., Collins, S.M., Peeters, T.L., 1999. Region-specific antiproliferative effect of VIP and PACAP-(1-38) on rabbit enteric smooth muscle. Am. J. Physiol. 276 (1 Pt. 1), G303–G310.

Vaudry, D., Falluel-Morel, A., Bourgault, S., Basille, M., Burel, D., Wurtz, O., Fournier, A., Chow, B.K., Hashimoto, H., Galas, L., Vaudry, H., 2009. Pituitary adenylate cyclase-activating polypeptide and its receptors: 20 years after the discovery. Pharmacol. Rev. 61 (3), 283–357. https://doi.org/10.1124/pr.109.001370.

Waschek, J.A., 2013. VIP and PACAP: neuropeptide modulators of CNS inflammation, injury, and repair. Br. J. Pharmacol. 169 (3), 512–523.